

Probing Glass Transition of Ultrathin Polymer Films at a Time Scale of Seconds Using Fast Differential Scanning Calorimetry

Mikhail Yu. Efremov, Eric A. Olson, Ming Zhang, Zishu Zhang, and Leslie H. Allen*

Department of Materials Science and Engineering and Coordinated Science Laboratory, University of Illinois at Urbana–Champaign, Urbana, Illinois 61801

Received December 15, 2003; Revised Manuscript Received April 9, 2004

ABSTRACT: Ultrasensitive, thin-film, differential scanning calorimetry is used to determine the glass-transition temperature of 3–400 nm thick, spin-cast films of polystyrene, poly (2-vinyl pyridine), and poly (methyl methacrylate) on a platinum surface. The technique used here is modified to characterize the glass transition over a time scale of seconds rather than milliseconds. No appreciable dependence of the glass transition temperature on thickness is observed over the entire range used. The results are discussed in comparison with previous calorimetric measurements, characterized by the glass-transition time scale of milliseconds.

1. Introduction

Gains made in manipulating and characterizing material on the microscale contribute significantly to modern science and industry, including microelectronics, medicine, and biology. Examination of glass transition in polymer films under 100 nm thick, particularly concerning dependence of glass-transition temperature T_g on film thickness, has attracted extensive attention.^{1–4} A vast variety of experimental methods—ellipsometry, Brillouin light scattering, X-ray reflectivity, positron lifetime spectroscopy, dielectric relaxation, local thermal analysis, AFM, etc.—have been utilized. However, the standard technique for glass-transition research in bulk materials—differential scanning calorimetry (DSC)—was not available for ultrathin polymer films until our recent advances in thin-film DSC (TDSC or “nanocalorimetry”).⁵ The importance of calorimetric measurements lies in the fact that it can measure fundamental thermodynamic properties such as heat capacity.

In our recent publication of nanocalorimetric investigations of polystyrene, poly (2-vinyl pyridine), and poly (methyl methacrylate) spin-cast films on a platinum surface, no appreciable dependence of glass-transition temperature over the thickness range from hundreds of nanometers down to 3 nm was observed.⁶ However, several other techniques, primarily ellipsometry, yield data which point to significant thickness dependence of T_g .^{1–4} The magnitude of the change of T_g with thickness in those experiments depends mostly on the type of polymer and substrate and typically achieves an increase or decrease of several tens of degrees of T_g from bulk samples down to about 10 nm thick films. One of our suppositions, which would make our calorimetric data consistent with results obtained by other methods, is that the absence of size dependence of T_g in nanocalorimetric experiments may be related to the high heating and cooling rates.⁶ These rates are 20–200 K/ms for heating and about 1–2 K/ms for cooling in the glass-transition region of the investigated polymers (100–200 °C). Nanocalorimetric data are

* To whom correspondence should be addressed. E-mail: L-ALLEN9@uiuc.edu.

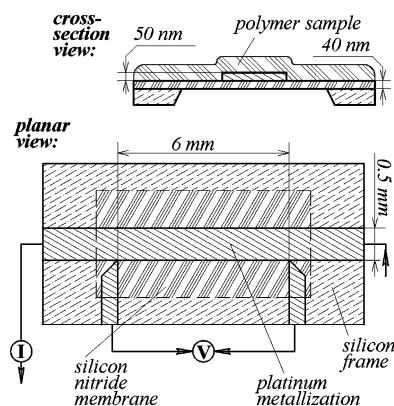


Figure 1. Cross-section and planar views of a typical TDSC sensor with a polymer sample on it (not to scale).

acquired upon heating. These high rates are inherent in the TDSC technique. In contrast, most other techniques take measurements on time scales on the order of seconds and minutes, not milliseconds.

To check this hypothesis, we make a special modification of the nanocalorimetry technique, which was briefly described elsewhere.⁵ The idea is to probe thermophysical properties (by nanocalorimetry) of polymer films as a function of annealing temperature. Annealing the sample immediately before the calorimetric scans can be made at time scales compatible with those of ellipsometric and other low scanning-speed techniques. In this case, the data from nanocalorimetric scans are used only as an indicator of changes in the sample when the annealing temperature reaches the glass-transition region. A similar approach was used, for example, in the study of glass transition on the surface of poly(vinyl alcohol) by sum-frequency vibrational spectroscopy.⁷

2. Experimental Section

2.1. Nanocalorimetry Technique. The nanocalorimetric technique is discussed in detail elsewhere.^{8–10} Briefly, our nanocalorimetric sensor (Figure 1) consists of a thin, free-standing, silicon nitride membrane (40–400 nm thick and several millimeters in height and width) supported by a silicon frame. Sensors with thick membranes are used for thick (70–80 nm and above) polymer films in order to resist the internal

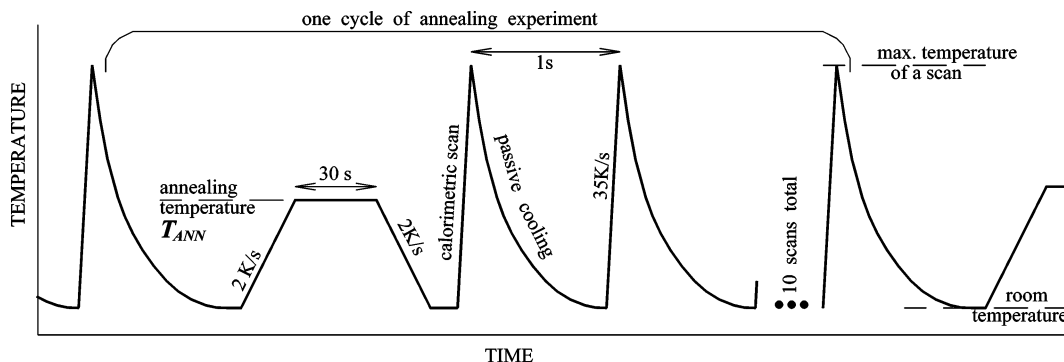


Figure 2. Structure of the annealing experiment.

stress in silicon nitride/polymer system. A platinum heater strip (~ 50 nm thick) is deposited onto one side of the membrane. By inducing a current through it, such a heater serves both to heat the membrane and to simultaneously measure its temperature. The heater's resistance is calibrated against temperature prior to the experiments. Very fast heating, varied from 20 to 200 K/ms, allows the sensor to operate in nearly adiabatic conditions. The calorimetric cell, consisting of thin membrane and heater strip only, has exceptionally low addenda, which is a key attribute of the high sensitivity of this method.

In the differential scheme, one sensor, used *as is*, serves as the reference one; the sample is placed on another sensor. During the experiment, a current pulse passes through the heaters of the sample and reference simultaneously. Differential voltage ΔV between the sample and reference sensors along with the voltage and current across the heaters are measured and used for power and temperature calculations and, finally, for calculation of $C_p(T)$, also known as the calorimetric curve.

2.2. Heat Capacity Analysis. Methods for heat capacity calculation using voltage and current experimental data are discussed in detail in ref 9. To obtain general calorimetric data for the samples in this investigation, the more accurate "main" method with three corrections⁹ is used. This method is useful, for example, to measure the amount of the polymer on the sensor (in the calorimetric cell). However, for processing of calorimetric scans in the annealing experiments, the simplified method is used. As emphasized in ref 9, the derivative of the differential voltage ΔV over time, $d\Delta V/dt$, contains the major part of the information about thermal processes in the sample. Heat capacity of the sample as a function of temperature $C_p(T)$ can be well approximated by the linear transformation of the $d\Delta V/dt(T)$ dependence, and all three corrections add relatively smooth terms (in comparison with $d\Delta V/dt(T)$ function) to the $C_p(T)$ dependence. This means that if the purpose of the measurement is to trace *changes* in the thermal properties of the sample caused by changes in the sample treatment (but not to quantify the properties), the $d\Delta V/dt(T)$ function will be as useful as the accurate $C_p(T)$ dependence. Moreover, in this case of using TDSC technique only as a probe of changes caused by different annealing procedures, the $d\Delta V/dt(T)$ function as a data output has advantages over $C_p(T)$. The accuracy of the "main" method of $C_p(T)$ calculations with the corrections comes at a price of complicated data treatment, which introduces additional spurious signals in the output. While the overall accuracy of the result is enhanced, the quality of separation between outputs for the measurements under close, but not identical, conditions, can be deteriorated. Additionally, the simplicity and quick turnaround of $d\Delta V/dt(T)$ calculation is essential in the measurements presented here, where typically 400 dependencies are analyzed and compared for each film sample.

2.3. Sample Preparation. Three types of monodispersed atactic polymer were chosen for this work: polystyrene, $M_w = 120\,200$, $M_w/M_n = 1.04$ (PS), poly(2-vinyl pyridine), $M_w = 138\,000$, $M_w/M_n = 1.30$ (PVP), and poly(methyl methacrylate), $M_w = 105\,400$, $M_w/M_n = 1.04$ (PMMA). To observe

effects of different molecular weight, several experiments with high molecular weight polystyrene, $M_w = 10\,200\,000$, $M_w/M_n = 1.22$ (PS-H), were performed. All samples were obtained from Polymer Source, Inc. These glass-forming polymers are widely used for studies of glass transition in thin films⁴ and were used in our previous direct nanocalorimetric studies.⁶ Annealing experiments were part of nanocalorimetric experiments discussed in ref 6, so the sample preparation and testing procedure are described there. In short, the films of polymers were formed by the spin-cast method from polymer solutions on the platinum heater of the calorimetric sensor. Film thickness was controlled both by varying the concentration of solution (0.06–7.5%) and the speed of rotation (3000–10 000 rpm, typically 10 000 rpm). Solvent used for PS and PMMA was toluene, and for PVP it was *n*-butanol. The average thickness of film on the heater was calculated from the room temperature heat capacity value, using the specific heat capacity of the bulk substance.

Additionally, the local film thicknesses on the heater at 15 points were measured (both before and after calorimetric measurement) *ex situ* by focused ellipsometry (Focus Ellipsometer FE-III, Rudolph Technologies, Inc) with a spot size of $12 \times 24 \mu\text{m}$. The deviation of any local thickness from the average value does not exceed $\pm 10\%$ except for the thickest (56 nm) PS-H sample. The agreement between both calorimetric and ellipsometric types of thickness measurements in 90% cases is better than $\pm 10\% \pm 0.2$ nm. The roughness of selected samples of PS, PVP, and PMMA on sensors was measured by atomic force microscopy (Digital Instruments Dimension 3000) after all calorimetric and ellipsometric measurements. The roughness of the thinnest films (1–2 nm) on the heater is equal to the roughness of the bare heater itself—about 1.5 nm of rms value. The roughness of thicker films decreases gradually with thickness. The AFM measurements also confirm that all polymers wet the surface of the platinum heater. After spin casting the polymer and taking ellipsometry measurements, the samples were preannealed in a vacuum for 1000 s at 140 °C for PS and PVP and at 160 °C for PMMA to maintain reproducibility of the thermal properties of the films throughout the whole experiment. Experiments were performed under high vacuum ($1-4 \times 10^{-8}$ Torr).

2.4. Experimental Procedure. The procedure of annealing measurement is illustrated in Figure 2. After the end of a previous cycle, the sample was heated 2 K/s up to the specific annealing temperature, T_{ANN} , isothermally annealed at this temperature for 30 s, and then cooled to room temperature at 2 K/s. Within a few seconds after the cooling period, 10 consecutive nanocalorimetry scans were performed at 1 s intervals. The scans were made starting from room temperature up to 240 °C for PS and PVP and up to 260 °C for PMMA, with heating rates of 30–40 K/ms. After reaching the maximum temperature during each scan, the sample was passively cooled at a rate of 1–2 K/ms over the 200–100 °C range (where the glass transition occurs). After the last scan, the annealing measurement is repeated at different T_{ANN} .

The lower limit of T_{ANN} was 30 °C, and the upper limit of T_{ANN} is 140 °C for PS and PVP and 200 °C for PMMA. During the experiment, T_{ANN} was changed monotonically by fixed

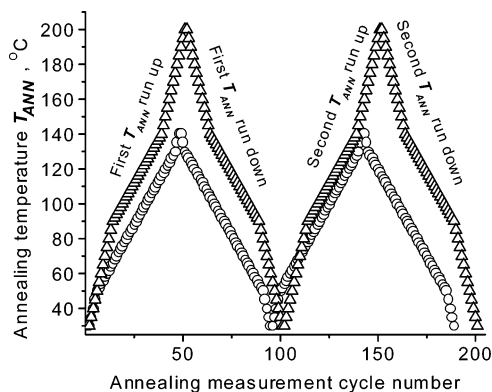


Figure 3. Schedule of T_{ANN} change during the annealing experiment: (Δ) PMMA, (\circ) PS and PVP.

increments/decrements from the lower limit to the upper limit (T_{ANN} run up) and back to the lower limit (T_{ANN} run down). Such large cycles were repeated twice. Increments of T_{ANN} were 5 K far away from glass-transition region and 2 K close to it. The schedule of T_{ANN} changes during the experiment is illustrated in Figure 3.

The calorimetric data are sensitive to tiny differences in the thermal history. For example, the data from the first scan after annealing is sensitive to the time interval between the end of the annealing procedure and the start of the scan. Because of this, the entire sequence of annealing cycles of a measurement (typically about 200 cycles of annealing–scanning) was done in a fully automatic regime to ensure adequate reproducibility of the thermal treatment of the sample.

2.5. Temperature Nonuniformity Over the Calorimetric Cell during the Annealing Procedure. The temperature regulation for the annealing procedure was performed by changing the current through the metal heater strip of the sensor. While the heating speed for a calorimetric scan is high enough to ensure practically adiabatic conditions and good uniformity of the temperature distribution within the calorimetric cell, slow heating during the annealing procedure is far from adiabatic and the temperature distribution within the calorimetric cell is significantly broader. The obvious consequence of the temperature nonuniformity during the annealing procedure is the broadening of the glass-transition region and, therefore, more uncertainty in the T_g assignment.

To estimate the nonuniformity of the temperature distribution over the calorimetric cell during the isothermal part of annealing, finite element modeling of the isothermal regime was performed. The modeling software was made on the basis of the Partial Differential Equation Toolbox of MATLAB software (release 12).¹¹ The model consists of the system of two equations—the Laplace elliptic equation for electrostatics of conductive media problem and the elliptic version of the heat balance equation for the steady-state conditions. Each equation was discretized by the finite element method, using meshes with more than 10^5 triangles and an adaptive mesh refinement algorithm.

Predefined parameters of the model are the sensors' dimensions, the experimentally measured electrical conductivity of the heater, the experimental temperature coefficient of metallization resistance, and the lateral heat conductivity of the platinum metallization of the sensors, estimated using the measured electrical conductivity of the metallization and the Wiedemann–Franz law. Heat conductivity of the polymer was neglected. The variable model parameters are the lateral heat conductivity of the silicon nitride membrane and the emissivity of the metallization. Emissivity of the membrane and polymer is assumed to be zero. It is also supposed that all heat conductivity and emissivity parameters do not depend on temperature. The variable parameters were fitted to satisfy the dependencies of the experimental heater temperature (measured via the heater resistance) versus electrical current through the heater for two types of sensors (with thin about 40 nm membranes and thick about 400 nm membranes).

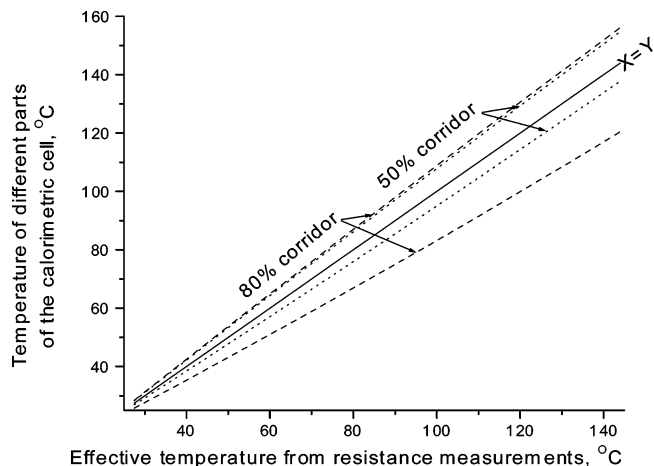


Figure 4. Temperature distribution over the calorimetric cell as a function of experimentally measured temperature of the heater.

The system of the equations is solved using an iterative procedure as follows. First, the electrostatic equation is solved and the distribution of the Joule heat sources over the metallization is found. Taking into account the Joule heat source distribution and the emissive heat loss, calculated on the basis of the temperature distribution from the previous cycle, the heat balance equation is solved. According to the new temperature distribution, the conductivity of the metallization is refined and the cycle is repeated. The solution procedure is complete when the results converge (typically after a few iterations).

The calculated distribution of the temperature over the calorimetric cell as a function of experimentally measured temperature of the heater (and sample) is illustrated in Figure 4. The nonuniformity of the temperature distribution becomes more pronounced with increasing temperature, but even at 140 °C (the maximal T_{ANN} for both PS and PVP) the experimental temperature gives practically nonshifted estimation of the median of the temperature distribution and more than 50% of the sample have the temperature within the range of ± 20 K of the experimental temperature.

3. Results and Discussion

In each annealing measurement (see Figure 2) the calorimetric curve from the first scan after annealing (1stS curve) is, in general, different from the subsequent nine scans (2ndS curves). The difference between the 1stS curve and all 2ndS curves reflects the different thermal histories of the sample. Each calorimetric scan heats the sample well above the glass transition, and such heating “erases” the thermal history of the sample. The 1stS curve reflects a thermal history that includes both passive cooling prior to annealing and the annealing procedure itself (Figure 5b). The 2ndS curves from scans, which immediately follow the passive cooling from a previous scan, reflect a thermal history that includes only passive cooling from the glass-transition region to room temperature (Figure 5a). Consequently, all scans which do not follow the annealing procedure (as in Figure 5a) give the same 2ndS curve throughout the whole experiment, regardless of annealing procedures and their conditions. In contrast, 1stS curves depend on T_{ANN} . If $T_{\text{ANN}} \ll T_g$ (as in Figure 5b), the 1stS calorimetric curve will be close to the 2ndS ones (type I of the 1stS curve). If $T_{\text{ANN}} > T_g$ (as in Figure 5c), the previous thermal history will be erased and the scan after annealing will probe the sample with a history of cooling from the glass-transition region down to the room temperature with the rate of 2 K/s (type II of the

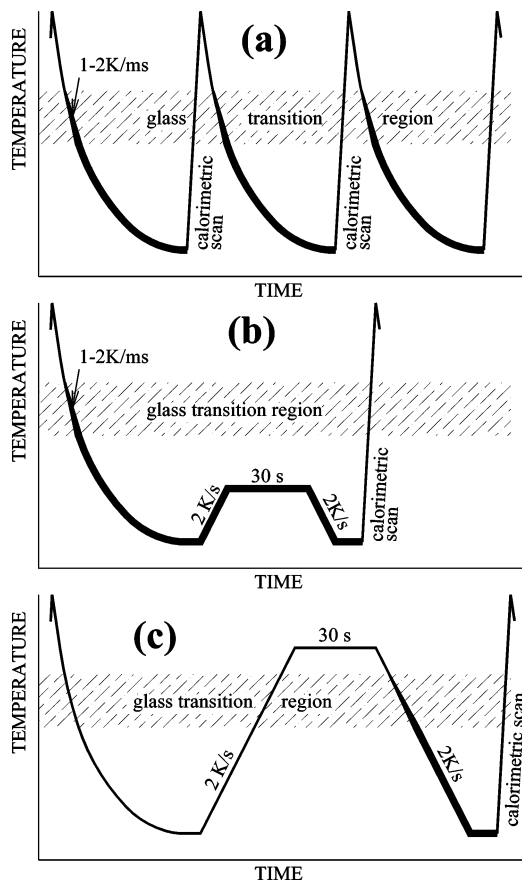


Figure 5. Different thermal histories of the sample for the calorimetric probe. Thick part of the curve denotes the region where the thermal history of the sample forms.

1stS curve). When T_{ANN} approaches T_g , the 1stS curve will have features of both types I and II. Summarizing, the temperature of transition between type I and type II 1stS curves with change of T_{ANN} can be used for the assignment of T_g of the sample. Moreover, the T_g assigned in this way will reflect the properties of the sample on the time scale of the annealing procedure, not the time scale of the calorimetric scan. In this case, nanocalorimetry is used only as an indicator of changes in sample properties influenced by T_{ANN} , not as a direct tool to assign T_g as a temperature of a feature on a $C_p(T)$ curve.

A typical series of the calorimetric curves is shown in Figure 6. As noted in section 2.2, in the case of annealing measurements, the thermal properties of the sample are presented as $d\Delta V/dt(T)$ functions rather than $C_p(T)$ dependencies. For our analysis, the use of $d\Delta V/dt(T)$ dependency is equivalent to the use of $C_p(T)$, and we will use the term "calorimetric curve" for $d\Delta V/dt(T)$ function also. A series made using both monotonic increasing and decreasing of T_{ANN} are essentially the same, and repetition of these series gives the same result.

To assign a value of T_g , we need to quantify the changes of the calorimetric curves when T_{ANN} changes: T_g in this approach would correspond to the change of the calorimetric curve as a whole when T_{ANN} crosses the glass-transition region. The parameter characterizing the curves should be a scalar that is sensitive to changes in the glass transition during the previous annealing procedure and is not sensitive to random deviations or noise in the signal. We found three parameters which satisfy these requirements.

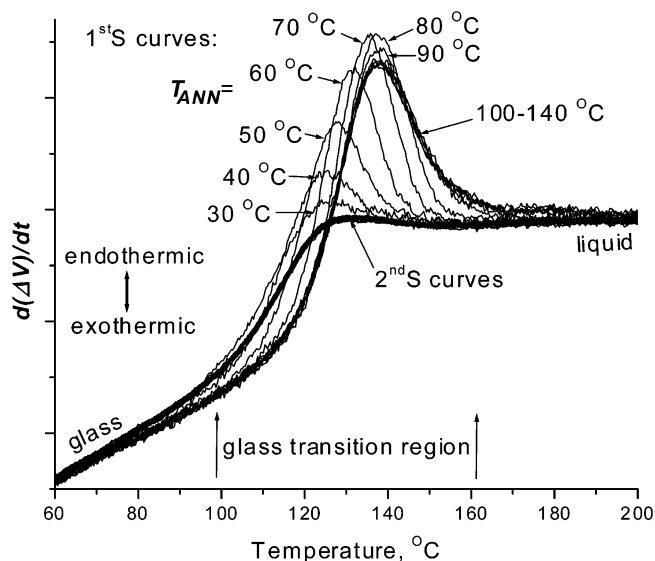


Figure 6. Series of calorimetric 1stS and 2ndS curves for T_{ANN} changing monotonically from 140 °C down to 30 °C. Sample: 3.5 nm thick PS film. Curves are smoothed for clarity by 51-point second-order polynomial Savitzky–Golay filter. Curves for selected T_{ANN} are shown only.

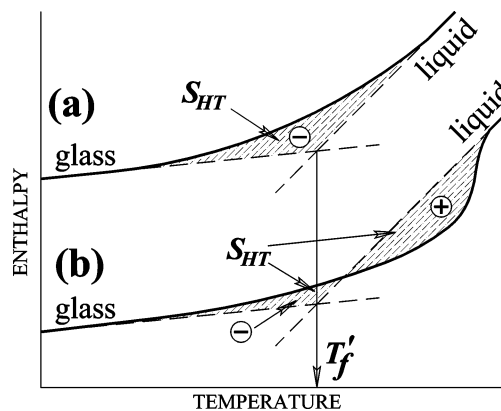


Figure 7. Limiting fictive temperature T'_f and "hysteresis integral" S_{HT} definition. Two cases are illustrated: (a) "classic" glass transition with the step on $C_p(T)$ curve and (b) glass transition with the hysteresis peak on $C_p(T)$ curve. "+" and "-" denote signs of terms which form S_{HT} .

One of these parameters is the limiting fictive temperature T'_f of the glass transition seen in a 1stS calorimetric curve. T'_f is defined as the temperature of the intersection of the extrapolated equilibrium liquid and glass $\Delta H(T)$ curves.¹² This construction is illustrated in Figure 7. T'_f can be calculated by the following equation

$$\int_{T_{MIN}}^{T'_f} (C_P - C_{PG})dT + \int_{T'_f}^{T_{MAX}} (C_P - C_{PL})dT = 0 \quad (1)$$

where T_{MIN} is any temperature below the glass-transition region and T_{MAX} is any temperature above it, C_{PG} is the glassy-state heat capacity, and C_{PL} is the liquid-state heat capacity, both extrapolated to T'_f . In our calculations we use $d\Delta V/dt(T)$ instead of heat capacity.

Another parameter, the "hysteresis integral" S_{HT} , can be found using the following equation

$$S_{HT} = \int_{T_{MIN}}^{T'_f} (C_P - C_{PG})TdT + \int_{T'_f}^{T_{MAX}} (C_P - C_{PL})TdT \quad (2)$$

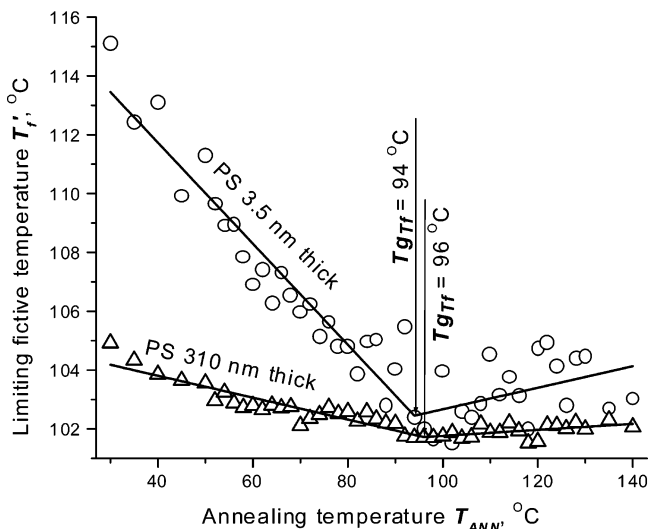


Figure 8. Dependence of T_f' for 1stS curves on T_{ANN} : (○) data for 3.5 nm thick PS film, (△) for 310 nm thick PS film. Straight lines denote linear fit.

This equation is invariant relative to shifts of temperature scale, so T can be either absolute or relative (for example, °C) temperature. According to eq 2, S_{HT} has the geometrical meaning of the signed area between the experimental $\Delta H(T)$ curve from the extrapolated equilibrium liquid and glass $\Delta H(T)$ curves. It is illustrated in Figure 7. As with T_f' , the $d\Delta V/dt(T)$ function is used for S_{HT} calculation instead of heat capacity.

The last parameter T_{PEAK} is the temperature of the peak on a 1stS calorimetric curve.

Typical dependencies of T_f' , calculated from 1stS curves, on T_{ANN} are shown in Figure 8. For T_{ANN} below the glass-transition region, T_f' decreases with increasing T_{ANN} . It is well known that T_g decreases with an increase in the extent of the annealing treatment.¹³ When T_{ANN} exceeds T_g , T_f' stabilizes—sample “forgets” the thermal history created before being cooled through the glass-transition region. This change of $T_f'(T_{ANN})$ behavior when T_{ANN} crosses the glass-transition region can be used to assign T_g . We will call T_g assigned in this way T_{gT_f} . Numerically, $T_f'(T_{ANN})$ is fitted by two intersected lines in the least-squares sense. The position of intersection gives us the T_{gT_f} value. This method is illustrated in Figure 8. We reiterate that the T_{gT_f} value reflects the glass transition over the time scale of the annealing procedure (seconds), in contrast to the shown T_f' values, which reflect the time scale of TDSC scans (milliseconds).

The dependence of T_{gT_f} on sample thickness for all investigated polymers is shown in Figure 9. The T_{gT_f} values for all polymers are significantly lower than T_f' , due to the difference in the time scales. Values of T_f' calculated from regular nanocalorimetric measurements using eight different heating rates in the 20–200 K/ms heating range are shown elsewhere,⁶ and the average values can be found in Table 1. Here, for illustration, the T_f' values calculated from 1stS curves with $T_{ANN} = 30$ °C are shown in Figure 10. The accuracy of T_f' shown in Figure 10 is significantly less than that demonstrated in ref 6, due to smaller statistics, the use of only one heating rate, and neglecting the extensive data corrections used in the accurate methods. However, the data in Figure 10, similar to the data in ref 6, show the same magnitude of T_f' and no significant T_g –thickness dependence for the given thickness range. (The jump in

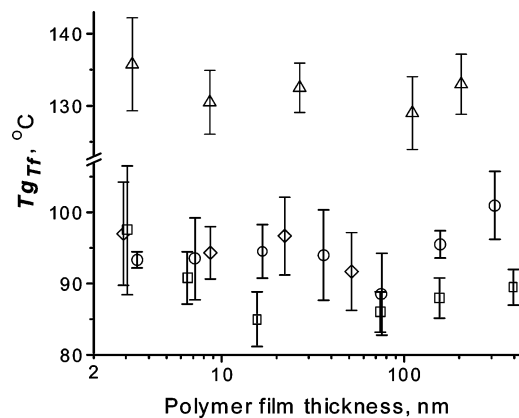


Figure 9. T_g assigned using 1stS curves T_f' data (T_{gT_f}) as a function of polymer film thickness: (○) PS, (◇) PS-H, (□) PVP, (△) PMMA. Error bars represent the standard deviation of four measurements (six for PS-H).

Table 1. T_g Assigned by Different Methods

| method of T_g assignment | T_g (in °C) for polymers | | | |
|---|----------------------------|------|-----|------|
| | PS | PS-H | PVP | PMMA |
| T_f' from regular nanocalorimetry measurements using eight different heating rates ^{a,6} | 114 | 112 | 111 | 145 |
| T_f' from annealing measurements, $T_{ANN} = 30$ °C, estimate values, this paper ^a | 110 | 115 | 104 | 136 |
| T_{gT_f} , this paper ^a | 94 | 96 | 90 | 132 |
| T_{gSHT} , this paper ^a | 93 | 95 | 90 | 134 |
| $T_{gT_{PEAK}}$, this paper ^a | 91 | 90 | 84 | 120 |
| T_f' for bulk samples, conventional DSC ¹⁴ | 99 | 102 | 94 | 128 |

^a Averages for all investigated film samples starting from 3 nm thickness and thicker.

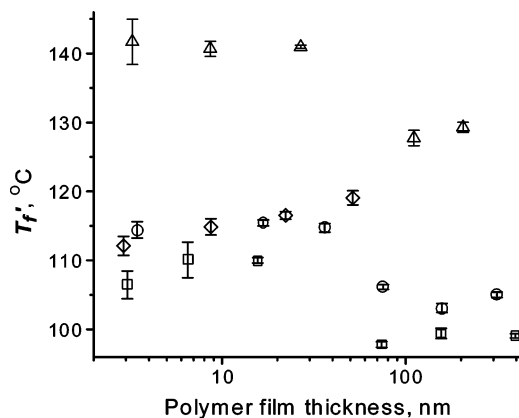


Figure 10. T_f' calculated from 1stS curves for $T_{ANN} = 30$ °C as a function of polymer film thickness: (○) PS; (◇) PS-H, (□) PVP, (△) PMMA. Error bars represent the standard deviation of four measurements (six for PS-H).

T_f' , which appears around a thickness of 70 nm, corresponds apparently to sensors with thicker membranes, used for thick films (see section 2.1). However, the reason of this jump is not clear.) On the other hand, T_{gT_f} are close to the bulk values determined by commercial DSC¹⁴—see Table 1. No appreciable dependence of T_{gT_f} on film thickness from a few nanometers up to several hundred nanometers can be seen in Figure 9. The same phenomenon—no T_g thickness dependence—was observed for millisecond time scale T_f' data.⁶ It allows us to suppose that the absence of a T_g thickness dependence is not characteristic of high heating and

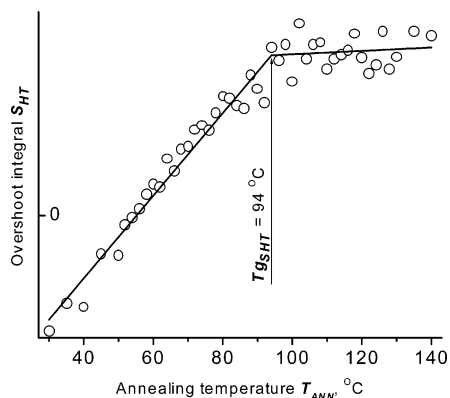


Figure 11. Dependence of hysteresis integral S_{HT} for 1stS curves on T_{ANN} . Sample: 3.5 nm thick PS film. Straight lines denote linear fit.

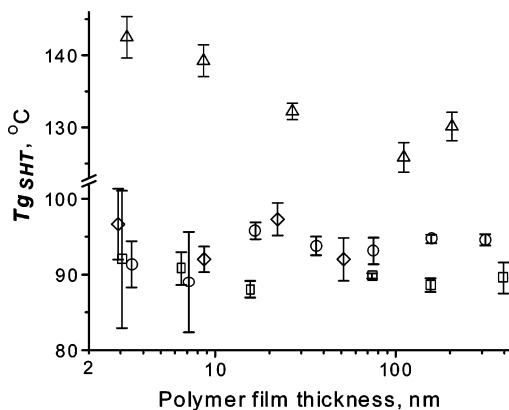


Figure 12. T_g assigned using 1stS curves S_{HT} data ($T_{gS_{HT}}$) as a function of polymer film thickness: (○) PS; (◇) PS-H, (□) PVP, (△) PMMA. Error bars represent the standard deviation of four measurements (six for PS-H).

cooling rates (or small time scale) but is a more general phenomenon.

There is the same situation for hysteresis integral S_{HT} . A typical dependence of S_{HT} , calculated from 1stS curves, on T_{ANN} is shown in Figure 11. For T_{ANN} below the glass-transition region, the overshooting (hysteresis peak, visible in Figure 6) on a calorimetric curve obtained from a DSC scan upon heating increases with increasing difference between cooling and subsequent heating rates or, equivalently, with increasing of the extent of the annealing treatment while the heating conditions remain the same.^{12,13} When T_{ANN} exceeds T_g , the calorimetric 1stS curve (and the hysteresis peak on it) stabilizes. As in the $T'_f(T_{ANN})$ case, this feature on a $S_{HT}(T_{ANN})$ function can be used to assign T_g , using the same method we described for $T_{gT'_f}$ (see Figure 11). We will denote T_g assigned using $S_{HT}(T_{ANN})$ as $T_{gS_{HT}}$.

The dependence of $T_{gS_{HT}}$ on sample thickness for all investigated polymers is shown in Figure 12. The $T_{gS_{HT}}$ values are close to $T_{gT'_f}$, shown in Figure 9, and also have no appreciable dependence on film thickness. $T_{gT'_f}$ for low thickness PMMA films slightly deviates both from $T_{gS_{HT}}$ for thicker films and from $T_{gT'_f}$ data. Supposedly this deviation is caused by increased error of $T_{gS_{HT}}$ evaluation for films with thickness below 10 nm, as the increased error bars for PS and PVP films suggest.

The $T_{gS_{HT}}$ data also support the conclusion made for $T_{gT'_f}$ that there is no appreciable thickness dependence of T_g for large (seconds) time scale DSC measurements.

The same discussion can be repeated for the T_{PEAK} parameter. A typical dependence of T_{PEAK} , calculated

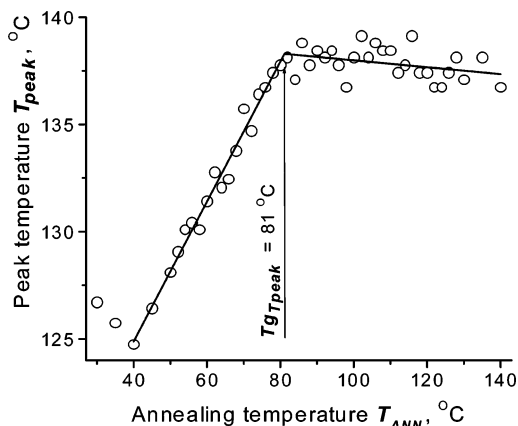


Figure 13. Dependence of the peak temperature T_{PEAK} for 1stS curves on T_{ANN} . Sample: 3.5 nm thick PS film, first run down. Straight lines denote linear fit.

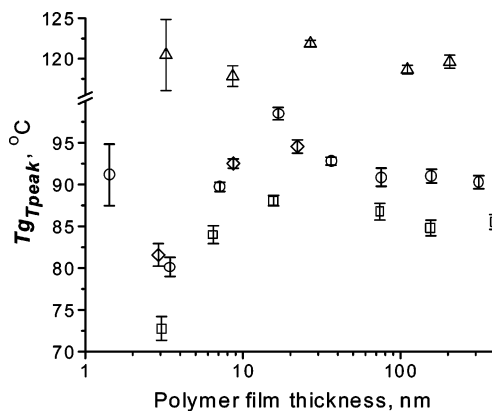


Figure 14. T_g assigned using 1stS curves T_{PEAK} data ($T_{gT_{PEAK}}$) as a function of polymer film thickness. (○) PS; (◇) PS-H, (□) PVP, (△) PMMA. Error bars represent the standard deviation of four measurements (six for PS-H).

from 1stS curves, on T_{ANN} is shown in Figure 13. As mentioned for S_{HT} , the hysteresis peak on a calorimetric curve increases with the extent of the annealing treatment. While T'_f is less susceptible to changes in thermal history, the increasing hysteresis peak should shift to higher temperatures in order to keep T'_f relatively constant. When T_{ANN} exceeds T_g , T_{PEAK} stabilizes. The same method, as for $T'_f(T_{ANN})$ and $S_{HT}(T_{ANN})$, can be used to assign T_g , as can be seen in Figure 13. The result will be denoted as $T_{gT_{PEAK}}$.

The dependence of $T_{gT_{PEAK}}$ on sample thickness for all investigated polymers is shown in Figure 14. $T_{gT_{PEAK}}$ for PMMA is about 10 K less than $T_{gT'_f}$ and $T_{gS_{HT}}$ values. There is no significant dependence of $T_{gT_{PEAK}}$ on film thickness, as in other two cases, but there is noticeable drop (about 10 K) in $T_{gT_{PEAK}}$ for PS, PS-H, and PVP at a film thickness of about 3 nm. It should be taken into consideration that while the first two parameters discussed above (T'_f and S_{HT}) are integral ones and incorporate information from the significant part of calorimetric curve, T_{PEAK} characterizes only a small part of the curve—the top of the glass-transition hysteresis peak—and, therefore, is less accurate. It also can be seen in Table 1 that average values of $T_{gT'_f}$ and $T_{gS_{HT}}$ are close to each other, but there is a noticeable difference between $T_{gT_{PEAK}}$ and both $T_{gT'_f}$ and $T_{gS_{HT}}$; additionally, both $T_{gT'_f}$ and $T_{gS_{HT}}$ values are closer to the bulk T_g than $T_{gT_{PEAK}}$ is.

Thus, for $T_{gT'_f}$, $T_{gS_{HT}}$, and $T_{gT_{PEAK}}$, no appreciable dependence on film thickness is found for these mea-

measurements on the time scale of seconds. Small, on the order of 10 K, deviations in $T_{gT_{PEAK}}$ for some polymers may be attributed to decreased reliability of T_g assignment using T_{PEAK} data.

Returning to the initial problem addressed by this work, it should be noted that one of the main results of our previous work⁶ is the absence of a dependence of T_g on the film thickness down to a few nanometers. This conclusion is the result of the investigation of supported PS, PS-H, PVP, and PMMA films on a platinum surface by the nanocalorimetric technique. On the other hand, ellipsometric measurements (which became de facto the standard method for investigation of T_g thickness dependence in supported polymer films), dielectric measurements, and several other methods show significant dependence of T_g on film thickness. One of the ideas devoted to explain this discrepancy considers the difference in the time scale of the glass transition investigated by nanocalorimetry and by ellipsometry. High heating rates, intrinsic to the TDSC method, make the time scale of the observed glass transitions on the order of milliseconds. Indeed, assuming a temperature interval of a glass transition of about 40 K and using a typical TDSC heating rate of 20–200 K/ms, the time of crossing the glass-transition region is 0.2–2 ms. A typical rate of temperature change in ellipsometric measurements is 0.2–2 K/min^{15–17} and in dielectric measurements is 0.5–3 K/min.^{15,18,19} These rates correspond with a glass-transition time scale of minutes. Hartmann and coauthors²⁰ show explicitly on the example of spin-cast i-PMMA films that, for the thickness range from the bulk down to 20 nm, the dependence of the maximum τ_{max} of the relaxation time distribution on the film thickness (activation plots) is negligible for $\tau_{max} \approx 0.1$ –1 ms. Thickness dependence of τ_{max} became pronounced when τ_{max} approaches the magnitude of seconds and more. Clearly, these results lead to the supposition that a glass-transition temperature on a milliseconds time scale would have negligible thickness dependence and became more pronounced for time scales of seconds and minutes.

Apparently, the results presented here do not support this hypothesis. The time scale of the glass-transition phenomenon in the annealing experiments can be estimated from the heating/cooling rate in the annealing treatment, 2 K/s. Using the same glass-transition interval as we used above, 40 K, the time scale of the glass-transition process in the presented experiments is about 20 s, which is more than four orders of magnitude greater than the time scale in the previous nanocalorimetric measurements. The absence of the T_g thickness dependence in both cases is an argument against the supposition mentioned above.

Literature data on the calorimetry of the small-sized samples of polymers used in this work are very limited but consistent with our results. A recent calorimetry study of small PS spheres in aqueous suspensions,²¹ where the authors overcome spurious coalescence effects, shows no substantial depression of T_g of PS spheres for the investigated range of diameters 42–548 nm. Adsorbed PS on silica with an equivalent average thickness estimated as 0.8–2 nm, investigated by a modulated DSC technique, demonstrates only a slight rise of T_g , 4–6 K above the bulk T_g .²² Interestingly, this increase in T_g probably corresponds with the increased (10–15 K) T_g for the smallest (1–1.5 nm) samples in our nanocalorimetry work.⁶

A reasonable explanation of this seeming contradiction—that some experimental methods show a significant T_g depression in thin polymer films while other ones, including calorimetry, do not—has appeared in recent publications by Forrest,¹ Porter and Blum,²² and Kawana and Jones¹⁷ and can be formulated as follows. While the temperature of a first-order thermodynamic transition (e.g., the melting of a crystal) can be measured, the glass-transition temperature T_g , due to the dynamic nature of glass transition, can only be assigned. The assignment of T_g using the concept of limiting fictive temperature T_f' , which was described above, depends only on the equilibrium liquid and glass enthalpy–temperature dependencies, so it is not sensitive to complex relaxation phenomena in the vicinity of the glass transition and is widely used both in experimental and theoretical works.^{12,13,23} Both our previous work with nanocalorimetry⁶ and the calorimetry of small PS spheres²¹ use this assignment to observe T_g –thickness dependence; the calorimetry of adsorbed PS uses a T_g definition which should yield values very close to T_f' for the presented calorimetric curves.

Other methods typically use arbitrary features of the experimental curves to assign T_g . We can expect that certain T_g assignments are more sensitive to the onset of the glass transition.²² These procedures yield values of T_g^{onset} , which can be close to other assignments and to T_f' , if the breadth of glass transition is small. Numerous investigations^{1–4} including the previously mentioned calorimetry works on nanoscale PS objects^{6,22} demonstrate pronounced broadening of glass transition with decreasing film thickness. The broadening effect obviously causes a low-temperature shift of the beginning of the glass transition and, consequently, the T_g^{onset} depression, even if T_f' is constant. For the ellipsometry technique and PS spin-coated films it is shown that T_g assigned as the onset temperature of the expansivity–temperature function demonstrates significant depression with decreasing thickness while the endpoint temperature of the glass-transition, $T_g^{endpoint}$, remains constant or slightly increases.¹⁷

Interestingly, a simple computational experiment demonstrates the same trends for T_g^{onset} and $T_g^{endpoint}$. Using the standard Tool–Naraswamy–Moynihan (TNM) model,⁵ we calculate $T_f'(T)$ function for virtual samples: bulk PS and PS films with different thicknesses d . Thermal history starts at $T_{MAX} = 240$ °C (when the samples are liquid); the virtual samples are cooled to $T_{MIN} = 20$ °C (when the samples are glassy) with the rate $v_{cooling} = -2$ K/s and then heated to T_{MAX} with the rate $v_{heating} = 2$ K/s. Parameters for bulk PS modeling are taken from ref 23 Table 1, using average values for the polymer: activation enthalpy $\Delta h^*/R = 76$ kK, stretch exponent $\beta_\infty = 0.69$, nonlinearity parameter $x = 0.48$, and limiting fictive temperature $T_{f\infty}' = 100$ °C. This set of values defines the fourth TNM parameter, the exponent coefficient A_{EXP} ($\log A_{EXP} = -87.53$, A_{EXP} given in seconds). We assume that film samples have bulk values of $\Delta h^*/R$, x , and A_{EXP} . The broadening of the glass transition in film samples with decreasing of d is introduced as a thickness dependence of the stretch exponent value, which characterizes the broadness of the relaxation time spectrum corresponding with glass transition: $\beta(d) = \beta_\infty \exp(-a/d)$, where $a = 4.9$ nm.⁶ Limiting the fictive temperature for the film samples, $T_f'(d)$ changes with $\beta(d)$. For T_g assignment, we use the heating part of the thermal history

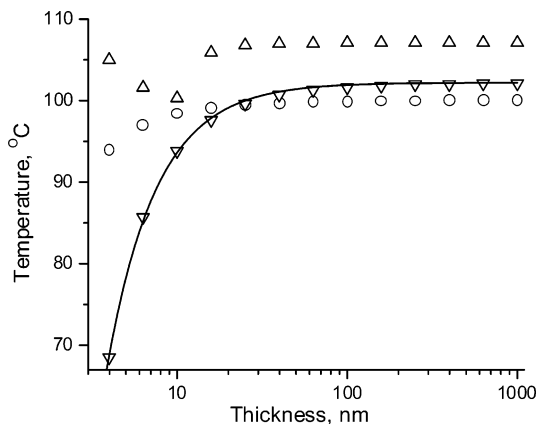


Figure 15. Output of the computational experiment with virtual PS films: T_g assigned by different methods as functions of film thickness d : (○) $T_g'(d)$, (△) $T_{g,\text{endpoint}}$, (▽) $T_{g,\text{onset}}$. Solid line denotes the best fit for $T_{g,\text{onset}}(d)$ dependence using the equation $T_{g,\text{onset}}(d) = T_{g,\text{onset}}(1 - (A/d)^\delta)$. The best-fit parameters are $A = 0.8$ nm, $\delta = 1.5$.

and two straightforward criteria. We assign $T_{g,\text{onset}}$ as the upper limit of the interval $[T_{\text{MIN}}, T]$ where the fictive temperature T_f is close to its glass value T_f' : $|T_f - T_f'| < 1$ K, and $T_{g,\text{endpoint}}$ as the lower limit of the interval $[T, T_{\text{MAX}}]$ where T_f approaches the real temperature T (this is characteristic for the liquid state): $|T_f - T| < 1$ K. The result is shown in Figure 15. Even for this simplistic model and rather arbitrary criteria for $T_{g,\text{onset}}$ and $T_{g,\text{endpoint}}$, we can see the same trends as discussed above: while T_f' is slightly decreasing with a decrease in d , $T_{g,\text{endpoint}}$ remains almost constant and $T_{g,\text{onset}}$ falls significantly. Note that the $T_{g,\text{onset}}$ trend is well-fitted by the standard empirical function for T_g depression: $T_g(d) = T_{g,\infty}(1 - (A/d)^\delta)$, where $T_{g,\infty}$ is T_g bulk value, A and δ are fitting parameters.²⁴ The best fit A and δ parameters are close to the literature values: compare $A = 0.8$ nm from our data and 0.83 nm from ref 25, $\delta = 1.5$ from our data and literature values 1.1,¹⁷ 1.8,²⁴ and 2.0.²⁶ The data obtained do not depend on the cooling/heating rate when $v_{\text{heating}} = -v_{\text{cooling}}$; any factor will change only the scaling parameter A_{EXP} .

In a conclusion, recent experimental works and even simple modeling supports the hypothesis that the experimental T_g trend depends on the type of T_g assignment and reflects the broadening of glass transition rather than a shift of the transition region.

Some publications have experimental procedures that are described in sufficient detail to show whether the T_g assignment used in a given work yields $T_{g,\text{onset}}$. One excellent example is the work²⁷ where so-called local thermal analysis is employed to observe the glass transition in PS, PMMA, and some other polymeric spin-cast films. The authors²⁷ state explicitly that T_g is assigned using the onset on the property–temperature diagrams. Moreover, the authors make another T_g assignment using the standard ellipsometry measurements and find that both methods agree and show the same T_g depression. In our opinion, this is more evidence that standard ellipsometry-based T_g assignment is biased to the beginning of glass transition. It is also shown²⁷ that the T_g values assigned in these ways for thick films are in agreement with bulk DSC measurements, which supports our supposition that $T_{g,\text{onset}}$ for bulk samples, where the glass-transition region is relatively narrow, can be close to the results obtained by traditional methods. Another example, where T_g

seems to be assigned close to the onset and shows a depression trend in a good agreement with ellipsometry measurements, is the work in ref 28; the thermal stress of the PS on Si is measured against temperature, and corresponding diagrams show details of the T_g assignment method.

In contrast, the method of T_g assignment used in the present work relies instead on the endpoint of the glass transition, where liquefying of the sample erases its thermal history. A similar approach is used in ref 7: poly(vinyl alcohol) samples with a mechanically treated surface are annealed and sum-frequency vibrational spectroscopy (SFS) is used to test whether the annealing erases the traces of the treatment. It is found that surface T_g is essentially the same as the bulk one.

The annealing approach described here is not limited to nanocalorimetry or SFS. It would be interesting to use the annealing experiments in combination with the techniques, which show T_g depression (ellipsometry, etc.). We suppose that these experiments would also yield more flat $T_g(d)$ dependencies.

It also should be noted that T_g assignment for extremely thin films typically yields less reliable results in comparison with thicker films. Besides the poor signal-to-noise ratio typical for minuscule samples, there are several other effects that complicate the T_g assignment in thin films. The phenomenon of loss of glass-transition contrast in thin films has already been used to resolve controversies in thin-film T_g studies.² Limited temperature range of glass-transition observation and curvature of the property–temperature plots outside of glass-transition region are discussed elsewhere.¹⁷ These effects can contribute a significant part in apparent trend of T_g –thickness dependence.

Several other interesting results of presented annealing experiments should also be mentioned. All three T_g versus thickness plots (Figures 9, 12, and 14) demonstrate no noticeable difference in T_g among polystyrene of a different molecular weight (PS and PS–H). The same phenomenon—the absence of T_g dependence on the molecular weight—was shown for the same polymers for calorimetric experiments with millisecond time scales.⁶ This phenomenon is commonly supported by glass-transition investigations of thin polymer films on substrates.¹

It is worth noting that the annealing experiments discussed here may serve as a sensitive technique to observe glass transitions in ultrathin polymer films, where regular nanocalorimetry measurements give doubtful results. Annealing experiments we have shown here are characterized by an extremely high ratio of heating and cooling rates, about 2×10^4 . In these conditions, the overshooting peak corresponded to the glass transition becoming significantly more pronounced than in the regular nanocalorimetric measurements, which have heating/cooling rate ratios of about 10–40 in the 100–200 °C temperature range. Figure 16 demonstrates that the glass transition in a 0.8 nm thick PVP film is hardly visible on a regular nanocalorimetric curve (2ndS curve) while the annealing 1stS curve gives clear evidence of the existence of the glass transition in this sample. Note that the given thickness of 0.8 nm is only an average value, measured in this case by ellipsometric measurements. A roughness of 1.5 nm (see section 2.3) means that the value of 0.8 nm cannot be treated as a local film thickness.

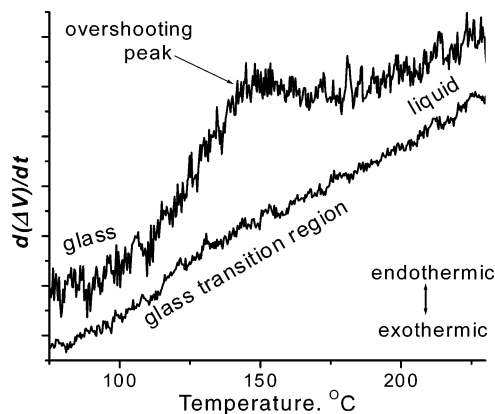


Figure 16. Calorimetric 1stS (upper) and 2ndS (lower) curves for PVP film with average thickness of about 0.8 nm. $T_{\text{ANN}} = 80$ °C. Curves are smoothed for clarity by 31-point second-order polynomial Savitzky–Golay filter. The 2ndS curve is the average of eight scans. The heating/cooling rate ratio is about 25 for 2ndS curve and about 20 000 for 1stS curve. Curves offset for clarity.

Our attempts to fit measured calorimetric curves using the TNM model, as we did in our previous works,^{5,6} were not successful. While fitting of $C_p(T)$ obtained by different scan rates and the same cooling history gives reasonable results, the fitting of calorimetric curves obtained using identical heating but different cooling histories (different T_{ANN}) meets serious problems. Figures 6, 8, 11, and 13 show that the shape of the 1stS calorimetric curves and their characteristic parameters change starting at the lowest T_{ANN} , 30 °C, and the parameters change almost linearly up to T_g . This behavior suggests a broad distribution of characteristic relaxation times with a smeared maximum(s). In contrast, fitting narrow and pronounced hysteresis peak upon heating gives a relatively narrow relaxation time spectrum (i.e., parameter β in the stretched exponent form of the relaxation function is close to 1), especially for thick films.^{5,6} This may indicate the lack of thermorheological simplicity²³ in the case of combining data from very different time scales in the same fit: the shape of the relaxation time distribution effectively changes when we go from the annealing procedure with a time scale of seconds to the nanocalorimetric scan with a time scale of milliseconds. We expect that broad time-scale nanocalorimetry, which is under development, would address this intriguing issue.

4. Conclusions

The glass-transition temperature T_g is measured in thin films of PS, PS–H, PVP, and PMMA polymers in the thickness range from hundreds of nanometers down to a few nanometers. A modification of the TDSC method is used in which the calorimetric curves are recorded as a function of the maximal annealing temperature T_{ANN} of the annealing treatment of the film tested. The T_g is assigned as an annealing temperature where the behavior of calorimetric curves with respect to T_{ANN} changes. Three parameters are used to represent changes in the curves with T_{ANN} : limiting fictive temperature T_f' , hysteresis integral S_{HT} , and peak temperature T_{PEAK} .

T_g assigned by this method corresponds to the time scale of the glass transition, which is different from the time scale of glass transition investigated by the regular TDSC technique, used in previous work.⁶ The regular

TDSC technique is characterized by high heating rates (20–200 K/ms); in the calorimetric scan, the sample crosses the glass-transition region in about 1 ms or less. The annealing modification to the TDSC technique gives the characteristics of the glass transitions that occurred during the annealing treatment of the sample; the calorimetric curves are used only as an indicator of changes in the state of the sample caused by annealing. Consequently, T_g obtained by the annealing modification of TDSC represents the time scale of the annealing treatment, which is seconds in this investigation. This time scale is close to the time scale of conventional DSC calorimeters—seconds or minutes.

Regardless of more than 3 orders of magnitude difference between the time scales of the regular and modified TDSC technique, the annealing measurements give essentially the same results as regular TDSC. No appreciable dependence of T_g on film thickness from hundreds of nanometers down to 3 nm is found for all investigated polymers. No molecular weight dependence of T_g is observed for polystyrene films. The difference in absolute values of T_g between these two methods is apparently explained by the difference in the heating/cooling rate ratio for each of these techniques.

Additionally, the annealing modification of the TDSC exaggerates the overshooting peak, typical for glass transition under high heating/cooling rate ratio conditions. This effect can be used to observe glass transition in extremely thin films, where the regular TDSC gives indistinct results.

Acknowledgment. We gratefully acknowledge P. Infante of CNF at Cornell University for assistance in the fabrication of the sensors and S. Granick and P. Geil from the University of Illinois at Urbana–Champaign for valuable discussions. We also greatly benefited from helpful discussions with J. Forrest from the University of Waterloo, Canada, who attracted our attention to ref 20 and the importance of time scale considerations. This work is supported by the US NSF-DMR 0108694 and ACS-PRF #37027-AC7. The calorimetry equipment was developed under NSF 9803019.

References and Notes

- (1) Forrest, J. A. *Eur. Phys. J. E* **2002**, *8*, 261.
- (2) Forrest, J. A.; Dalnoki-Veress, K. *Adv. Colloid Interface Sci.* **2001**, *94*, 167.
- (3) McKenna, G. B. *J. Phys. IV Fr.* **2000**, *10*, Pr7–53 and Pr7–343.
- (4) Forrest, J. A.; Jones, R. A. L. In *Polymer Surfaces, Interfaces and Thin Films*; Karim, A., Kumar, S., Eds.; World Scientific: Singapore, 2000; p 251.
- (5) Efremov, M. Yu.; Warren, J. T.; Olson, E. A.; Zhang, M.; Kwan, A. T.; Allen, L. H. *Macromolecules* **2002**, *35*, 1481.
- (6) Efremov, M. Yu.; Olson, E. A.; Zhang, M.; Zhang, Z.; Allen, L. H. *Phys. Rev. Lett.* **2003**, *91*, 085703.
- (7) Zhang, C.; Hong, S.-C.; Ji, N.; Wang, Y.-P.; Wei, K.-H.; Shen, Y. R. *Macromolecules* **2003**, *36*, 3303.
- (8) Olson, E. A.; Efremov, M. Yu.; Zhang, M.; Zhang, Z.; Allen, L. H. *MEMS J.* **2003**, *12*, 355.
- (9) Efremov, M. Yu.; Olson, E. A.; Zhang, M.; Lai, S. L.; Schiettekatte, F.; Zhang, Z. S.; Allen, L. H. *Thermochim. Acta* **2004**, *412*, 13.
- (10) Efremov, M. Yu.; Olson, E. A.; Zhang, M.; Schiettekatte, F.; Zhang, Z. S.; Allen, L. H. *Rev. Sci. Instrum.* **2004**, *75*, 179.
- (11) *Partial Differential Equation Toolbox User's Guide*; The MathWorks, Inc.: Natick, MA, 1995.
- (12) Moynihan, C. T. In *Assignment of the Glass Transition*, ASTM STP 1249; Seyler, R. J., Ed.; American Society for Testing and Materials: Philadelphia, 1994; p 32.

- (13) Wunderlich, B. In *Assignment of the Glass Transition, ASTM STP 1249*; Seyler, R. J., Ed.; American Society for Testing and Materials: Philadelphia, 1994; p 17.
- (14) T_g' for bulk quantity of used substances is measured using Perkin-Elmer DSC7, calibrated against the melting temperature of In and Ga; polymer samples are 5–20 mg, and data are collected during heating with rate 3 K/min.
- (15) Sharp, J. S.; Forrest, J. A. *Phys. Rev. E* **2003**, *67*, 031805.
- (16) Herminghaus, S.; Jacobs, K.; Seeman, R. *Eur. Phys. J. E* **2001**, *5*, 531.
- (17) Kawana, S.; Jones, R. A. L. *Phys. Rev. E* **2001**, *63*, 021501.
- (18) Fukao, K.; Miyamoto, Y. *Phys. Rev. E* **2000**, *61*, 1743.
- (19) Fukao, K.; Uno, S.; Miyamoto, Y.; Hoshino, A.; Miyaji, H. *J. Non-Cryst. Solids* **2002**, *307–310*, 517.
- (20) Hartmann, L.; Gorbatschow, W.; Hauwede, J.; Kremer, F. *Eur. Phys. J. E* **2002**, *8*, 145.
- (21) Sasaki, T.; Shimizu, A.; Mourey, T. H.; Thureau, C. T.; Ediger, M. D. *J. Chem. Phys.* **2003**, *119*, 8730.
- (22) Porter, C. E.; Blum, F. D. *Macromolecules* **2002**, *35*, 7448.
- (23) Hodge, I. M. *J. Non-Cryst. Solids* **1994**, *169*, 211.
- (24) Keddie, J. L.; Jones, R. A. L.; Cory, R. A. *Europhys. Lett.* **1994**, *27*, 59.
- (25) **A** is extracted from the review,¹⁷ Figure 1. The value presented in the caption of the figure (8.3 nm) is not correct. It should be decreased by a factor of 10, as our analysis of the figure suggests.
- (26) Ellison, C. J.; Torkelson, J. M. *Nat. Mater.* **2003**, *2*, 695.
- (27) Fryer, D. S.; Nealey, P. F.; de Pablo, J. J. *Macromolecules* **2000**, *33*, 6439.
- (28) Zhao, J.-H.; Kiene, M.; Hu, C.; Ho, P. S. *Appl. Phys. Lett.* **2000**, *77*, 2843.

MA035909R